Moving force identification from bending moment responses of bridge

Ling Yu[†] and Tommy H. T. Chan[‡]

*Department of Civil and Structural Engineering, The Hong Kong Polytechnic University,
Hung Hom, Kowloon, Hong Kong*

Abstract. Moving force identification is a very important inverse problem in structural dynamics. Most of the identification methods are eventually converted to a linear algebraic equation set. Different ways to solve the equation set may lead to solutions with completely different levels of accuracy. Based on the measured bending moment responses of the bridge made in laboratory, this paper presented the time domain method (TDM) and frequency-time domain method (FTDM) for identifying the two moving wheel loads of a vehicle moving across a bridge. Directly calculating *pseudo-inverse* (PI) matrix and using the singular value decomposition (SVD) technique are adopted as means for solving the over-determined system equation in the TDM and FTDM. The effects of bridge and vehicle parameters on the TDM and FTDM are also investigated. Assessment results show that the SVD technique can effectively improve identification accuracy when using the TDM and FTDM, particularly in the case of the FTDM. This improved accuracy makes the TDM and FTDM more feasible and acceptable as methods for moving force identification.

Key words: moving force identification; bridge-vehicle interaction; time domain method; frequency-time domain method; singular value decomposition; bending moment; response measurement.

1. Introduction

Moving force identification has been studied extensively in connection with the design of railway tracks and bridges. Accurate identification of moving forces experienced during operation is vital for accurate and cost effective design and maintenance of bridges. Determination of accurate force can not only lead to a great reliance on numerical simulation based upon analytical models, but also dramatically reduce the need for more expensive and time consuming experimental testing. In general, input forces to a system can be directly measured using load transducers. However, in some situations, the input locations may not be accessible for measurement. Therefore, the indirect identification of the input forces from the dynamic responses of the structures appears to be a valuable alternative.

The problem of moving force identification has been studied for a long time. Fryba (1972) presented a comprehensive survey of the references and methods for solving the problems involving

---

† PhD Student
‡ Associate Professor

moving loads on structures. The original "moving-mass moving-force" problem was approximated by the simplified "moving-force" problem by Timoshenko *et al.* (1974). Stevens (1987) provided an overview of the force identification process for the case of linear vibratory systems. A number of different applications of force identification were described, and the computational procedures and difficulties involved were outlined. Starkey and Merrill (1989) performed a careful error analysis on the acceleration method. They determined that the error in the predicted forces was largely dependent on the condition number of the coefficient matrix of equation set. Tang (1990) also discussed the precision problems of dynamic load identification in the time domain. Kammer (1998) presented a time domain method for estimating the discrete input forces acting on a structure based upon its measured response and employed a regularization technique to stabilize computations. Cao (1998) described the application of an artificial neural network to identify the loads distributed across a cantilevered beam.

Based on a system identification theory, the authors have developed another two moving force identification methods, namely the time domain method (TDM, Law *et al.* 1997) and the frequency-time domain method (FTDM, Law *et al.* 1999). Comparative studies (Chan *et al.* 2000c) showed that the two methods could identify moving forces with acceptable accuracy to some extent. The TDM was the best one, but the FTDM suffered from several constraints that mainly associated with the solution by applying the *pseudo-inverse* technique to the over-determined equation with a rank deficient coefficient matrix. The singular value decomposition (SVD) technique, applied to structural dynamics problems in the last fifteen years, is one of the most important tools in numerical analysis (Gloub *et al.* 1996 and Press *et al.* 1996). If the coefficient matrix A is close to rank deficient then the *pseudo-inverse* is best calculated from the singular value decomposition of A (Lindfield *et al.* 1995).

In this paper, a brief description of the TDM and FTDM is given first. Laboratory experiments are then introduced. The results of a comparative study showed the effects of the bridge and vehicle parameters on the TDM and FTDM. These results also demonstrated robustness of the adopted SVD technique to solve the over-determined system equation in the TDM and FTDM.

2. Theoretical background

The bridge superstructure is modeled with a simply supported beam with a span length L, constant flexural stiffness EI, constant mass per unit length ρ and viscous proportional damping C.
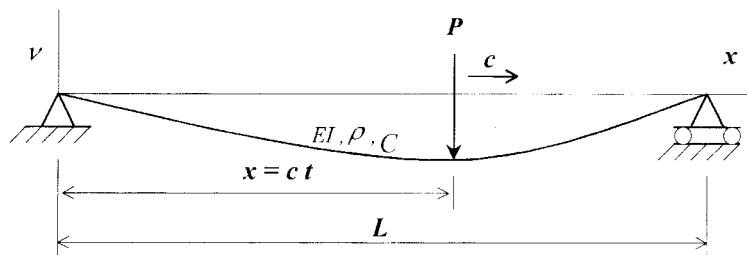

Fig. 1 Moving force on a simple supported beam

The effects of shear deformation and rotary inertia are not taken into account (Bernoulli-Euler beam). If the force P moves from left to right at a speed c, as shown in Fig. 1, then the equation of motion can be expressed as

$$\rho\frac{\partial^2 v(x, t)}{\partial t^2} + C\frac{\partial v(x, t)}{\partial t} + EI\frac{\partial^4 v(x, t)}{\partial x^4} = \delta(x - ct)P(t) \tag{1}$$

where $v(x, t)$ is the beam deflection at point x and time t and $\delta(x - ct)$ is the Dirac delta function. Based on modal superposition, if the nth mode shape function of the beam $\Phi_n(x) = \sin(n\pi x/L)$, the solution of Eq. (1) can be expressed as

$$v(x, t) = \sum_{n = 1}^{\infty} \sin\frac{n\pi x}{L}q_n(t) \tag{2}$$

where n is the mode number, $q_n(t)$, $(n = 1, 2, ..., \infty)$ are the nth modal displacements. After substituting Eq. (2) into Eq. (1), integrating the resultant equation with respect to x between 0 and L, and then using the boundary conditions and the properties of the Dirac delta function, the equation of motion in terms of the modal displacement $q_n(t)$ can be expressed as

$$\ddot{q}_n(t) + 2\xi_n\omega_n\dot{q}_n(t) + \omega_n^2 q_n(t) = \frac{2}{\rho L}p_n(t) \quad (n = 1, 2, ..., \infty) \tag{3}$$

where

$$\omega_n = \frac{n^2\pi^2}{L^2}\sqrt{\frac{EI}{\rho}}, \quad \xi_n = \frac{C}{2\rho\omega_n}, \quad p_n(t) = P(t)\sin\left(\frac{n\pi\bar{x}}{L}\right) \tag{4}$$

are the nth modal frequency, the modal damping and the modal force respectively. $\bar{x}$ is the distance of the axle from the left-hand support. If the time-varying force $P(t)$ is known, Eq. (3) can be solved to yield $q_n(t)$ and the dynamic deflection $v(x, t)$ can then be obtained from Eq. (2). This is called the forward problem. The moving force identification is an inverse problem in structural dynamics, in which the unknown time-varying force $P(t)$ is identified using the measured displacements, accelerations or bending moments of real structures. The TDM and FTDM have been developed for moving force identification.

2.1 Time domain method (TDM)

Eq. (3) can be solved in the time domain by the convolution integral and the dynamic deflection $v(x, t)$ of the beam at point x and time t can be obtained from

$$v(x, t) = \sum_{n = 1}^{\infty} \frac{2}{\rho L\omega_n'} \sin\frac{n\pi x}{L}\int_0^t e^{-\xi_n\omega_n(t - \tau)}\sin\omega_n'(t - \tau)\sin\frac{n\pi c\tau}{L}P(\tau)d\tau \tag{5}$$

where $\omega_n' = \omega_n\sqrt{1 - \xi_n^2}$. Therefore, the bending moment in the beam at point x and time t is

$$m(x, t) = -EI\frac{\partial^2 v(x, t)}{\partial x^2} = \sum_{n=1}^{\infty}\frac{2EI\pi^2 n^2}{\rho L^3 \omega_n'}\sin\frac{n\pi x}{L}\int_0^t e^{-\xi_n \omega_n (t-\tau)}\sin\omega_n'\,(t-\tau)\sin\frac{n\pi c\tau}{L}P(\tau)d\tau \quad (6)$$

Assuming that both the time-varying force $P(t)$ and the bending moment $m(x, t)$ are step functions in a small time interval Δt, Eq. (6) can be rewritten in discrete terms and rearranged into a set of equations

$$M_{N\times 1} = B_{N\times N_B}F_{N_B\times 1} \tag{7}$$

where, F is the time series vector of the time-varying force $P(t)$ and M is the time series vector of the measured bending moments in the bridge deck at point x. The coefficient matrix B is associated with the system of the bridge deck and the force. The subscripts $N_B = L/(c\Delta t)$ and N are the numbers of sample points for the force $P(t)$ and measured bending moment M respectively when the force moves across the whole bridge deck.

2.2 Frequency-time domain method (FTDM)

Eq. (3) can also be solved in the frequency domain. Performing the Fast Fourier Transform (FFT) on Eq. (3), the Fourier transform of the dynamic deflection $v(x, t)$ is

$$V(x, \omega) = \sum_{n=1}^{\infty}\frac{1}{M_n}\Phi_n(x)H_n(\omega)P_n(\omega) \tag{8}$$

where $M_n = \rho L/2$, $H_n(\omega)$ is the frequency response function of the nth mode, and

$$H_n(\omega) = \frac{1}{\omega_n^2 - \omega^2 + i2\xi_n\omega_n\omega} \tag{9}$$

$$\Phi_n(x) = sin(n\pi x/L) \tag{10}$$

$$P_n(\omega) = \frac{1}{2\pi}\int_{-\infty}^{\infty}p_n(t)e^{-i\omega t}dt \tag{11}$$

2.2.1 Force identification from accelerations
The Fourier transform of the acceleration of the beam at point x is obtained from Eq. (8) as

$$\ddot{V}(x, \omega) = -\omega^2\sum_{n=1}^{\infty}\frac{1}{M_n}\Phi_n(x)H_n(\omega)P_n(\omega) \tag{12}$$

Substituting Eqs. (9)-(11) into Eq. (12) and rewriting in discrete terms,

$$\ddot{V}(m) = -\sum_{k=0}^{N-1}\sum_{n=1}^{\infty}\frac{\Delta f^3 m^2}{M_n}\Phi_n(x)H_n(m)\Psi_n(m-k)F(k), \quad m = 0, 1, ..., N-1 \tag{13}$$

where Ψ_n is the Fourier transform of the nth mode shape, Δf is the frequency resolution in the FFT, N is the number of data samples in the FFT, k and m denote the kth and the mth term in the FFT and F is the Fourier transform of the moving force $P(t)$. Considering the periodic property of the

Discrete Fourier Transform (DFT) and letting

$$\overline{H}_{xn}(m) = -\frac{\Delta f^3 m^2}{M_n}\Phi_n(x)H_n(m) \tag{14}$$

then Eq. (13) can be rewritten in matrix form

$$\ddot{V}_{(N+2)\times 1} = A_{(N+2)\times(N+2)}F_{(N+2)\times 1} \tag{15}$$

where $\ddot{V}$ and F are Fourier transform of the acceleration vector $\ddot{v}$ and the force vector $P(t)$, respectively. The matrix A is associated with the bridge-vehicle system. Dividing F into real and imaginary parts F_R and F_I, respectively, Eq. (15) becomes

$$\ddot{V} = (A_{RR} + iA_{RI})F_R + i(A_{IR} + iA_{II})F_I \tag{16}$$

Similarly, Dividing $\ddot{V}$ into real and imaginary parts $\ddot{V}_R$ and $\ddot{V}_I$, it yields

$$\begin{Bmatrix} \ddot{V}_R \\ \ddot{V}_I \end{Bmatrix}_{(N+2)\times 1} = \begin{bmatrix} A_{RR} & -A_{II} \\ A_{RI} & A_{IR} \end{bmatrix}_{(N+2)\times(N+2)} \begin{Bmatrix} F_R \\ F_I \end{Bmatrix}_{(N+2)\times 1} \tag{17}$$

Since the first and last elements of the Fourier transform of the imaginary parts of vectors $\ddot{v}$ and P equal to zero, i.e., $\ddot{V}_I(0) = \ddot{V}_I(N/2) = 0$, $F_I(0) = F_I(N/2) = 0$, Eq. (17) can be condensed into a set of N-th order simultaneous equations by deleting corresponding rows and columns as

$$\ddot{V}_{RI} = A_D F_{RI} \tag{18}$$

Components F_R and F_I can be found from Eq. (18) by solving the N order set of linear equations. The time history of the moving force $P(t)$ can then be obtained by performing the inverse Fourier transformation. The solution is obtained in the frequency domain. However, the computation cost for solving Eq. (18) is high in finding the inverse of a full matrix, and therefore the following procedure is developed to overcome these difficulties.

If the DFTs are expressed in matrix form, the Fourier transform of the force vector F will be written as follows

$$F = \frac{1}{N}WP \tag{19}$$

where $W = e^{-i2k\pi/N}$ and all terms in F are real (Bendat *et al.* 1993).

$$k = \begin{bmatrix} 0 & 0 & 0 & \dots & 0 & 0 \\ 0 & 1 & 2 & \dots & N-2 & N-1 \\ 0 & 2 & 4 & \dots & N-4 & N-2 \\ \vdots & \vdots & \vdots & \ddots & \vdots & \vdots \\ 0 & N-2 & N-4 & \dots & 4 & 2 \\ 0 & N-1 & N-2 & \dots & 2 & 1 \end{bmatrix}_{N\times N} \tag{20}$$

The matrix W is an unitary matrix, which means

$$W^{-1} = (W^*)^T \tag{21}$$

where W^* is a conjugate of W.

Substituting Eq. (19) into Eq. (18), it yields

$$\ddot{V} = \frac{1}{N} A \underset{N \times N_B}{[W_B \quad 0]} \begin{Bmatrix} f_B \\ 0 \end{Bmatrix} \tag{22}$$

or

$$\underset{N \times 1}{\ddot{V}} = \frac{1}{N} \underset{N \times N}{A} \underset{N \times N_B}{W_B} \underset{N_B \times 1}{P_B} \tag{23}$$

Linking the Fourier transform of acceleration $\ddot{v}$ with the force vector P_B of the moving forces in the time domain. W_B and P_B are the sub-matrices of W and P respectively. $N_B = L/(c\Delta t)$ is the number of data samples for the force $P(t)$ on the beam. Using Eq. (23) for identification has the advantage of weighting the response data in the frequency domain, but the disadvantage is that the noise of the responses during the time interval $(N_B \Delta t)$ to $(N \Delta t)$ will affect the accuracy of the identified forces. Eq. (23) can be written using Eq. (19) to relate the accelerations and force vectors in the time domain as

$$\underset{N \times 1}{\ddot{v}} = \underset{N \times N}{(W^*)^T} \underset{N \times N}{A} \underset{N \times N_B}{W_B} \underset{N_B \times 1}{P_B} \tag{24}$$

If $N = N_B$, P_B can be found by solving the Nth order linear equations in Eq. (23) or (24). If $N > N_B$ or l accelerations are measured, the least squares method can be used to find the time history of the moving forces $P(t)$. If only $N_c (N_c \le N)$ response data points of the beam are used, the equations for these data points in Eqs. (23) and (24) can be extracted and described as

$$\underset{N_c \times 1}{\ddot{V}} = \frac{1}{N} \underset{N_c \times N_c}{A} \underset{N_c \times N_B}{W_B} \underset{N_B \times 1}{P_B} \tag{25}$$

$$\underset{N_c \times 1}{\ddot{v}} = \underset{N_c \times N}{(W^*)^T} \underset{N \times N}{A} \underset{N \times N_B}{W_B} \underset{N_B \times 1}{P_B} \tag{26}$$

In usual cases, $N_c > N_B$ and more than one acceleration measurement can be used to identify a single moving force for a higher accuracy.

2.2.2 Identification from bending moments

Similarly, the relationships between bending moment m and its Fourier transform M, and the moving force vector P can be described as follows

$$\underset{N \times 1}{M} = \frac{1}{N} \underset{N \times N}{B} \underset{N \times N_B}{W} \underset{N_B \times 1}{P_B} \tag{27}$$

$$\underset{N \times 1}{m} = \underset{N \times N}{(W^*)^T} \underset{N \times N}{B} \underset{N \times N_B}{W_B} \underset{N_B \times 1}{P_B} \tag{28}$$

$$\underset{N_c \times 1}{m} = \underset{N_c \times N}{(W^*)^T} \underset{N \times N}{B} \underset{N \times N_B}{W_B} \underset{N_B \times 1}{P_B} \tag{29}$$

The force vectors P_B can be obtained from the above three sets of equations by using the least squares method.

2.2.3 Two forces identification

The above procedures have been derived for single force identification. Further, Eq. (28) can be modified for two force identification using the linear superposition principle as

$$m = (W^*)^T \begin{bmatrix} B_a & 0 \\ B_b & B_a \\ B_c & B_b \end{bmatrix} W_B \begin{Bmatrix} P_1 \\ P_2 \end{Bmatrix} \tag{30}$$

where $B_a[N_s \times (N_B - 1)]$, $B_b[(N - 1 - 2N_s) \times (N_B - 1)]$ and $B_c[N_s \times (N_B - 1)]$ are sub-matrices of matrix B. The first sub-matrix row in the matrix B describes the state when only the first force is applied on the beam. The second and third sub-matrix rows respectively describe the states when two forces are on the beam and when the second force remains on the beam after the exit of the first force respectively. Similarly, as before, the two moving forces can be identified using more than one measured bending moment measurement.

2.3 Solutions

As mentioned above, it is easy to see that the TDM or the FTDM will usually result in a system of equations with the form

$$Ax = b \tag{31}$$

where, x is the time series vector of the unknown time-varying force $P(t)$, b is the time series vector of the measured bending moment response $m(x, t)$ or acceleration response $a(x, t)$ of the bridge deck at the point x. The system matrix A is associated with the bridge-vehicle system. Assuming its size is $k \times n$, where k and $n = L/(c\Delta t)$ are the numbers of sample points for the response $m(x, t)$ or $a(x, t)$ and for the force P respectively when the force goes across the whole bridge deck, if $k > n$, then the system $Ax = b$ is an over-determined system of equations. In principle, Eq. (31) will have a solution given by the least-squares method as

$$x = A^+ b = [(A^T A)^{-1} A^T] b \tag{32}$$

where A^+ denotes the *pseudo-inverse* (PI) of matrix A. The solution vector x is called the PI solution in Eq. (32). This definition requires A to have full rank. A^+ is an $n \times k$ array that is unique. If matrix A is square and non-singular then $A^+ = A^{-1}$, Eq. (31) becomes a linear equation system, and the force vector x can be directly found by solving Eq. (31). If matrix A is singular, Eq. (31) is ill-posed and the elements of the solution vector x will be sensitive to small changes in both matrix A and vector b. If matrix A is close to rank deficient then A^+ is best calculated from the singular value

decomposition (SVD) of A (Lindfield *et al.* 1995). The SVD technique, applied to structural dynamics problems in the last fifteen years, is one of the most important tools in numerical analysis (Gloub *et al.* 1996 and Press *et al.* 1996).

If matrix A is real, the SVD of A is USV^T, where, U and V are two orthogonal matrices, their sizes are $k \times k$ and $n \times n$, respectively. S is a real diagonal $k \times n$ matrix in which the elements at the leading diagonal of this matrix are called the singular values of A. Once the singular value decomposition of the matrix A is known, its inverse can easily be calculated from $A^+ = VS^{-1}U^T$. For simplicity, assuming that A has no exact zero singular values, it can be shown that the least-squares solution vector x is given by

$$x = \sum_{i=1}^{\min(k,n)} \frac{u_i^T b_i}{\sigma_i} v_i \qquad (33)$$

The solution vector x here is called the SVD solution. Eq. (33) clearly illustrates the difficulties associated with standard matrix solutions of Eq. (31). If the numerator does not decay as fast as the singular value σ_i of the denominator, the solution is dominated by terms containing the smallest σ_i. Consequently, the solution x may have many sign changes and thus appear to be random. When A is rank deficient, only the $r(r \leq \min(k, n))$ non-zero singular values of the matrix are taken into account so that S is a $r \times r$ matrix where r is the rank of A. To make the multiplication of Eq. (33) conformable, the first r columns of V and the first r columns of U in Eq. (33) are used.

3. Experiments in the laboratory

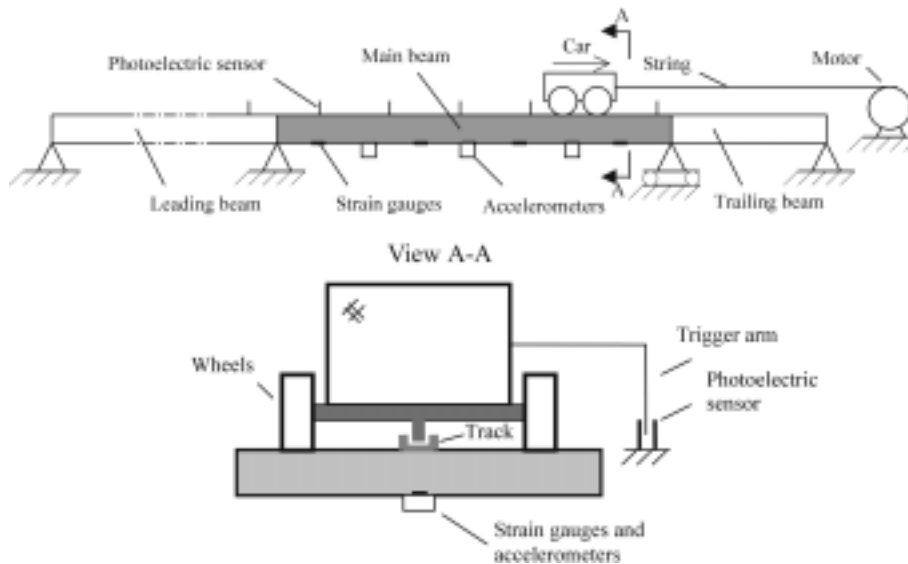A model car and a model bridge deck were constructed in the laboratory. An Axle-Spacing-to-

Fig. 2 Experimental setup of moving force identification

Span-Ratio (ASSR) is defined as the ratio of the axle spacing between two consecutive axles of the vehicle to the bridge span length. Here, the ASSR was set to be 0.15. The model car had two axles at a spacing of 0.55 m and was mounted on four rubber wheels. The static mass of the whole vehicle was 12.1 kg in which the real wheel mass was 3.825 kg. The model bridge deck, so called main beam as shown in Fig. 2, was simply supported between a leading beam and a trailing beam. On the leading beam a constant vehicle speed was reached as the model car approached the bridge deck. The trailing beam was used for decelerating the car. The main beam, with a span length of 3.678 m and 101 mm × 25 mm uniform cross-section, was made from solid rectangular mild steel bar with a density of 7335 kg/m^3 and a flexural stiffness $EI = 29.97$ kNm^2. The first three theoretical natural frequencies of the main beam were calculated as $f_1 = 4.5$ Hz, $f_2 = 18.6$ Hz, and $f_3 = 40.5$ Hz.

A U-shaped aluminum track was glued to the upper surface of the main beam as a guide way for the model car, which was pulled along by a string wound around the drive wheel of an electric motor. The speed of the motor could be adjusted. Seven photoelectric sensors were mounted on the beams to measure and check the uniformity of speed of the model car. Seven equally spaced strain gauges and three equally spaced accelerometers were mounted on the lower surface of the main beam to measure the response. A system calibration of the strain gauges was carried out, before the actual testing program, by adding masses at the middle of the main beam. A 14-channel tape recorder was employed to record the response signals. The first seven channels were used for logging the bending moment response signals from the strain gauges. Channels 8 to 10 were used for logging the accelerations from the accelerometers. Channel 11 was connected to the photoelectric sensors. In addition, the response signals from channels 1 to 7 and channel 11 were also recorded simultaneously on a PC for easy analysis. The software Global Lab from the Data Translation was used for data acquisition and analysis in the laboratory test. Before exporting the measured data in ASCII format for identification, the Bessel IIR digital filter with lowpass characteristics was implemented as cascaded second-order systems.

4. Comparative studies

This comparative study is aimed at investigating the effects of several bridge-vehicle systems parameters on TDM and FTDM methods as well as comparing the SVD solution in Eq. (33) with the PI solution in Eq. (32). The parameters studied include the sampling frequency, the mode number used, the speed of the vehicle, the measuring station numbers and locations. In practice, the parameters were studied one at a time. The procedure was to examine each parameter in the cases studied and to isolate the case with the highest accuracy for the corresponding parameter. The accuracy is quantitatively defined as Eq. (34), called a Relative Percentage Error (RPE).

$$RPE = \frac{\sum |f_{true} - f_{ident}|}{\sum |f_{true}|} \times 100\% \tag{34}$$

However, because the true forces are unknown, this is not practical. The true force (f_{true}) and identified force (f_{ident}) in Eq. (34) are here replaced by the measured response ($R_{measured}$) and rebuilt response ($R_{rebuilt}$) respectively (Chan *et al.* 2000a & b) in order to calculate the RPE between the measured and rebuilt responses instead of comparing the identified forces with the true forces

directly. In the comparative studies being reported here, the results were based on the measurements of bending moments. For each method, the identified forces were first calculated based on the bending moment response from all seven measuring stations. The rebuilt responses were then computed accordingly from the identified forces. The RPE values between the rebuilt and measured bending moment responses at each station were finally tested for validation of each identification method. The maximum acceptable RPE value adopted here is 10% (Chan *et al.* 2000c).

4.1 Effect of sampling frequency

In each laboratory experiment case, the response was acquired at a sampling frequency of 1000 Hz per channel. This frequency was higher than the practical demand because only a few first lower frequency modes are usually used in moving force identification. The sequential data points acquired at 1000 Hz were sampled again at a few intervals in order to obtain new sequential data at a lower sampling frequency. New sequential data at the sampling frequencies of 333, 250 and 200 Hz would be obtained by sampling the data again at every third, fourth and fifth point respectively. In the TDM and FTDM studies, the sampling frequency f_s should be high enough to ensure sufficient accuracy in the discrete integration. Because there is a computer memory problem in the computation of the inverse of a large matrix, the maximum sampling frequency is limited to be within 500 Hz,

Table 1 Effect of sampling frequency on TDM (15 Units, MN=5)

f_s	RPE (%)						
	sta. 1	sta. 2	sta. 3	sta. 4	sta. 5	sta. 6	sta. 7
333	4.62	2.62	1.68	1.91	1.78	2.58	3.08
	4.63*	2.63	1.68	1.95	1.80	2.58	3.08
250	5.43	3.09	1.80	2.56	1.94	3.43	4.83
	5.42	3.08	1.80	2.58	1.95	3.44	4.83
200	8.55	4.00	2.63	3.71	2.99	4.72	9.54
	8.55	4.00	2.62	3.72	2.99	4.72	9.55

*Underlined values are for the *pseudo-inverse* technique, the same applies to the following Tables.

Table 2 Effect of sampling frequency on FTDM (15 Units, MN=5)

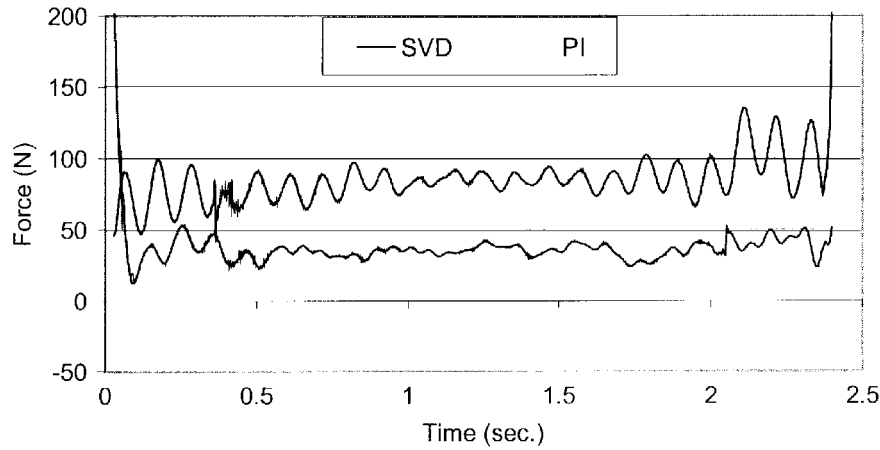| f_s	RPE (%)						
	sta. 1	sta. 2	sta. 3	sta. 4	sta. 5	sta. 6	sta. 7
333	4.51	2.53	1.87	1.95	1.82	2.25	3.17
	204.8	168.6	156.8	148.0	153.6	161.9	186.9
250	4.53	2.52	1.87	1.95	1.82	2.24	3.17
	5.74	2.80	2.15	2.08	2.14	2.41	4.74
200	4.51	2.53	1.87	1.95	1.82	2.25	3.17
	4.58	2.54	1.87	1.98	1.83	2.26	3.18

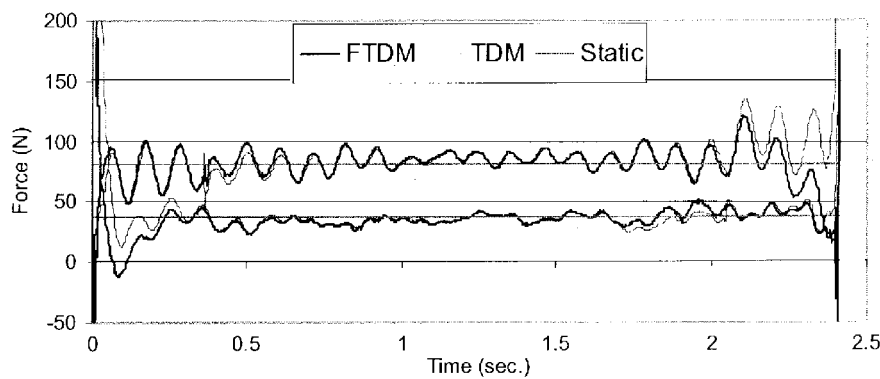Fig. 3 Identified forces by TDM using SVD & PI

Fig. 4 Identified forces by FTDM and TDM using SVD

and sampling frequencies of 200, 250 and 333 Hz were set here. The sampling frequency giving the highest accuracy will be adopted for the subsequent study of the effect of other parameters, i.e., the mode number (MN) used, the speed of the vehicle, the measuring station numbers and their locations. Tables 1 and 2 are for the TDM and FTDM respectively, in which the effect of the sampling frequency is taken into account, the RPE values between the measured and rebuilt bending moment are given for the SVD solution and the PI solution respectively. The case given is for MN=5, the sensor number is seven and the car speed is 15 Units (1 Unit $\cong$ 0.102 m/s).

Table 1 shows the identification accuracy that is acceptable for the TDM under all cases. The higher the sampling frequency, the lower are the RPE values for all stations. The TDM is suitable for the higher sampling frequency case. The highest identification accuracy corresponds to the highest sampling frequency f_s = 333 Hz. It can be observed from Table 1 that there is almost no difference for the RPE data at each station using the SVD or the PI technique. However, by studying Fig. 3, it can be predicted that the forces identified by the SVD are better than those by the PI. This occurs particularly at the moment that the second axle approaches the bridge when the first

axle is on the beam. It can be seen that the identified first forces by the PI have more random errors with higher frequency.

For the FTDM, Table 2 clearly shows the comparison of the identified results by the SVD and by the PI technique. When using the PI technique, the effect on the identification accuracy increases with the increase in the sampling frequency. When the sampling frequency is 333 Hz, the FTDM is failed because all the RPE values at seven stations are higher than 148%. When decreasing the sampling frequency to 250 Hz, further to 200 Hz, the FTDM is acceptable. This shows that the FTDM is suitable for a lower sampling frequency when the PI technique is used to solve the equation. The highest accuracy corresponds to the lowest sampling frequency case, i.e., $f_s = 200$ Hz, which is almost same accuracy as the SVD at this sampling frequency. Significantly, the identified results by the SVD are clearly different from those by the PI. They are almost constant at each station for the different sampling frequencies. This means that use of the SVD technique is independent to the sampling frequency. Further, use of the SVD can effectively improve the identification accuracy, especially when the sampling frequency is in the highest case 333 Hz.

When comparing Table 2 with Table 1, it can be found that the RPE data by the SVD are much closer when the highest sampling frequency $f_s = 333$ Hz is used. Fig. 4 shows the comparison of the

Table 3 Effect of mode number (MN) on TDM (15 Units, 250 Hz)

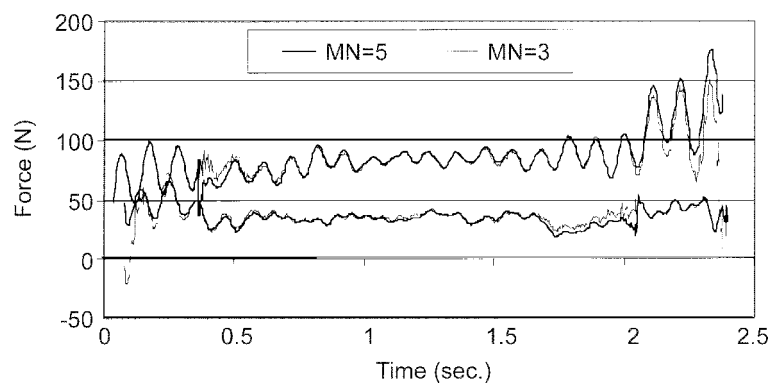| MN	RPE (%)						
	sta. 1	sta. 2	sta. 3	sta. 4	sta. 5	sta. 6	sta. 7
3	11.57	3.36	5.03	2.66	5.23	3.72	12.22
4	5.80	3.33	1.89	2.85	1.98	3.76	5.76
5	5.43	3.09	1.80	2.56	1.94	3.43	4.83
6	8.09	3.79	2.57	2.42	2.75	4.65	7.12
7	14.28	6.46	6.89	3.95	6.58	5.38	10.96
8	14.28	6.46	6.89	3.95	6.58	5.38	10.96
9	14.29	6.48	6.89	3.95	6.57	5.38	10.94
10	21.24	13.83	10.11	5.01	10.01	13.11	19.38

Fig. 5 Identified forces by TDM using SVD for MN=3 & MN=5

Table 4 Effect of mode number on FTDM (15 Units, 250 Hz)

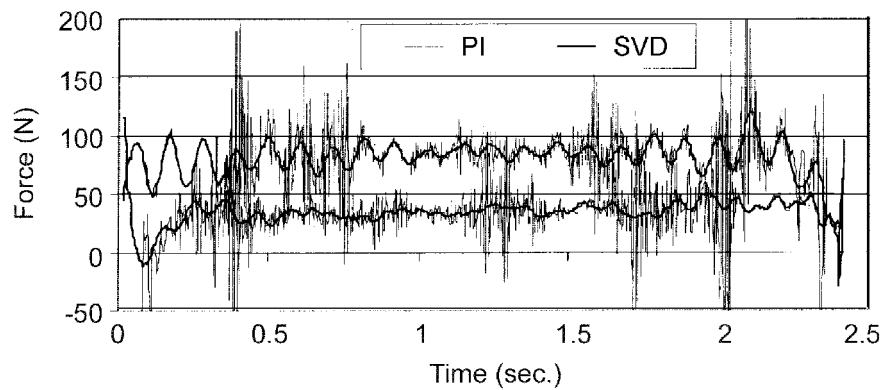| MN	RPE (%)						
	sta. 1	sta. 2	sta. 3	sta. 4	sta. 5	sta. 6	sta. 7
3	12.10	3.51	5.26	2.61	5.21	3.70	12.91
	Fail	Fail	Fail	Fail	Fail	Fail	Fail
4	5.88	3.24	2.03	2.64	1.97	3.55	5.83
	13.58	7.19	5.69	5.93	5.55	6.75	12.91
5	4.53	2.52	1.87	1.95	1.81	2.24	3.17
	5.74	2.80	2.15	2.08	2.14	2.41	4.74
6	3.74	2.57	1.77	1.95	1.58	1.62	2.06
	4.91	2.72	1.89	2.05	1.73	1.87	3.45
7	3.69	2.36	1.44	1.55	1.15	1.32	1.82
	4.79	2.44	1.54	1.73	1.39	1.57	3.07
8	3.69	2.36	1.44	1.55	1.16	1.32	1.82
	4.73	2.42	1.53	1.64	1.35	1.50	3.02
9	3.55	2.21	1.39	1.52	1.17	1.29	1.90
	4.59	2.30	1.50	1.63	1.30	1.49	3.20
10	3.41	1.85	1.28	1.50	1.03	0.92	1.63
	5.05	2.23	1.52	1.96	1.34	1.62	4.24

Fig. 6 Identified forces by FTDM using SVD & PI for MN=5

identified forces for the TDM and FTDM respectively when the SVD is used. It clearly illustrates the identified results are feasible and in a good agreement with each other, especially during the period when both the two axles of the car are on the beam.

4.2 Effect of mode number (MN)

The case $f_s = 250$ Hz, $c = 15$ Units is chosen for studying the effects of mode numbers. The mode
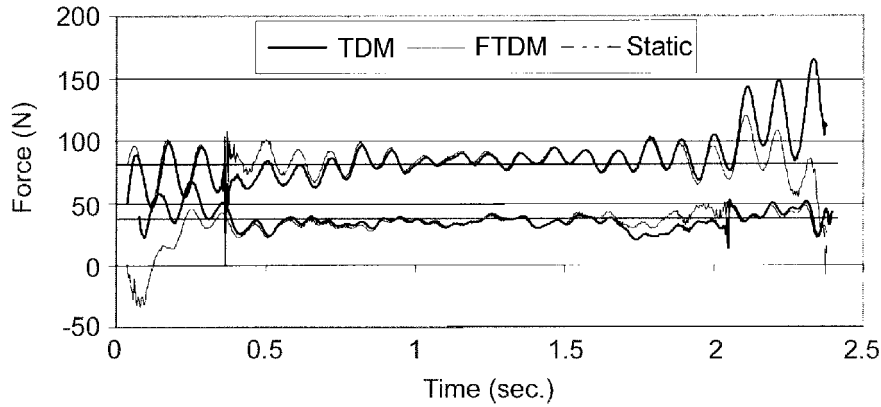
Fig. 7 Identified forces by FTDM & TDM using SVD for MN=4

number was varied from MN=3 to MN=10. Table 3 lists the RPE values for the TDM using the SVD. The results using the PI are not listed here because the accuracy is almost the same as that using the SVD except for the case MN=3. When MN=3 and using the PI technique, the TDM is not effective because the RPE values at all seven stations are higher than 100%. When MN=3 but using the SVD, the identified results are acceptable although are bigger RPE values than 10% at the 1st and 7th stations. This shows that the SVD technique can effectively improve the identification accuracy for the TDM. If the mode number is larger than 3, the RPE values increase gradually with the increase in the mode number. If the mode number increases up to MN=10, the TDM is again not effective at all measuring stations except station 4. By studying the RPE data in Table 3, it can be found that the best case is case MN=5. Fig. 5 illustrates the comparison of the identified forces when MN=3 and MN=5 respectively. The curve for MN=5 in Fig. 5 is clearly smoother and more feasible than that for MN=3.

The results for the FTDM are given in Table 4. They show that the RPE values decrease slightly with an increase in the mode number whether using the SVD or the PI technique. Further, comparing the data at each station, it can be seen that the result using the SVD is clearly improved in identification accuracy, particularly for the lower mode number cases MN=3 and MN=4. When MN=3 and using the PI technique, the FTDM fails, but using the SVD, the identified results are acceptable except that there are bigger RPE values than 10% at the 1st and 7th stations. When MN=4, using the SVD can effectively improve the identification accuracy by more than 50% at each station. This shows that using the SVD technique to solve the system equation can clearly improve the FTDM. Moreover, Fig. 6 illustrates the forces identified by the FTDM when using the SVD and the PI respectively. The curve in Fig. 6 illustrates that using the PI is less acceptable than using the SVD because it has components with higher frequency noise.

If the mode number is less than 3, both the RPE values and the identified forces become very poor and both the TDM and FTDM fail to identify the two moving forces. The above fact shows the two methods are effective only if the required mode number is achieved or exceeded. Further, use of the SVD can effectively improve the identification accuracy of the two methods, especially for the FTDM. From the data in Tables 3 and 4, it can be predicted that the FTDM is better than the TDM when using the SVD. As an example, the RPE data are very close to each other when MN=4 and using the SVD. The identified forces are illustrated in Fig. 7. The results by the FTDM are more

Table 5 Effect of vehicle speed on TDM and FTDM (MN=4, f_s = 200 Hz)

Station	RPE (%)					
	TDM			FTDM		
	5 − 2	10 − 4	15 − 2	5 − 2	10 − 4	15 − 2
1	5.18, 5.23	5.89, 5.89	6.72, 6.71	23.71, Fail	23.3, 110.	5.87, 5.94
2	3.46, 3.48	2.66, 2.66	3.31, 3.30	13.00, Fail	12.6, 50.0	3.24, 3.29
3	2.87, 2.88	2.95, 2.95	2.43, 2.42	6.79, Fail	7.99, 25.9	2.04, 2.05
4	3.30, 3.31	3.19, 3.20	2.99, 3.01	7.90, Fail	8.32, 48.2	2.65, 2.66
5	2.78, 2.80	2.76, 2.76	2.58, 2.58	6.93, Fail	7.79, 24.8	1.98, 2.01
6	4.20, 4.22	3.91, 3.91	3.96, 3.96	12.40, Fail	11.8, 47.6	3.55, 3.57
7	5.75, 5.78	7.38, 7.38	6.29, 6.29	26.37, Fail	26.3, 102.	5.84, 5.89

feasible than those by the TDM because they are closer to the two static axle weights, particularly for the identified first force between 0.4-0.8 seconds and the second force between 1.7-2 seconds.

4.3 Effect of vehicle speed

Three vehicle speeds were set manually at 5, 10 and 15 Units respectively in the experiments. After acquiring the data, the speed of the vehicle was calculated and the uniformity of the speed was checked. If the speed was stable, the experiment was repeated five times for each speed case to check whether or not the properties of the structure and the measurement system had changed. If no significant change was found, the corresponding recorded data were accepted for identification of the moving forces. After checking the speed of the vehicle between two triggers, it was found that apparent differences in the speed existed in each segment of the beam. Therefore, the average speed of the vehicle on the whole beam was assumed to identify the moving forces in the TDM and FTDM. In addition, some limitations on the TDM and FTDM have been first considered. In particular, a necessary RAM memory and CPU speed of the personal computer were required for both the TDM and FTDM. Otherwise, a significant amount of execution time is needed due to large size of the coefficient matrix A in Eq. (32), or they cannot be executed at all due to insufficient memory. If the mode number, the sampling frequency and bridge span length are not be changed in this case, a change of the vehicle speed would mean a change of the sampling point number, which will in turn change the dimensions of matrix A in Eq. (32). Therefore, in order to make the TDM and FTDM effective and to analyze the effects of various vehicle speeds on the identified results, the case with MN=4, f_s = 200 Hz was selected. The RPE values were calculated and tabulated in Table 5 for Cases 5-2, 10-4 and 15-2. Case "5-2" means the *second set* of data was recorded when the vehicle moved across the bridge at the speed 5 Units. Others are similarly identified. The data in Table 5 show that the TDM is effective for all three various vehicle speeds. The RPE data at each station are almost the same for each speed whether using the SVD or the PI technique. Although the change in the RPE value is not so significant, the RPE values tend to reduce with the increase in the vehicle speed, especially for those measuring stations with middle regions.

When using the PI technique, the FTDM failed to identify the forces when the vehicle speed is lower, says 5 Units, but the identified results get better and better as the vehicle speed increases.
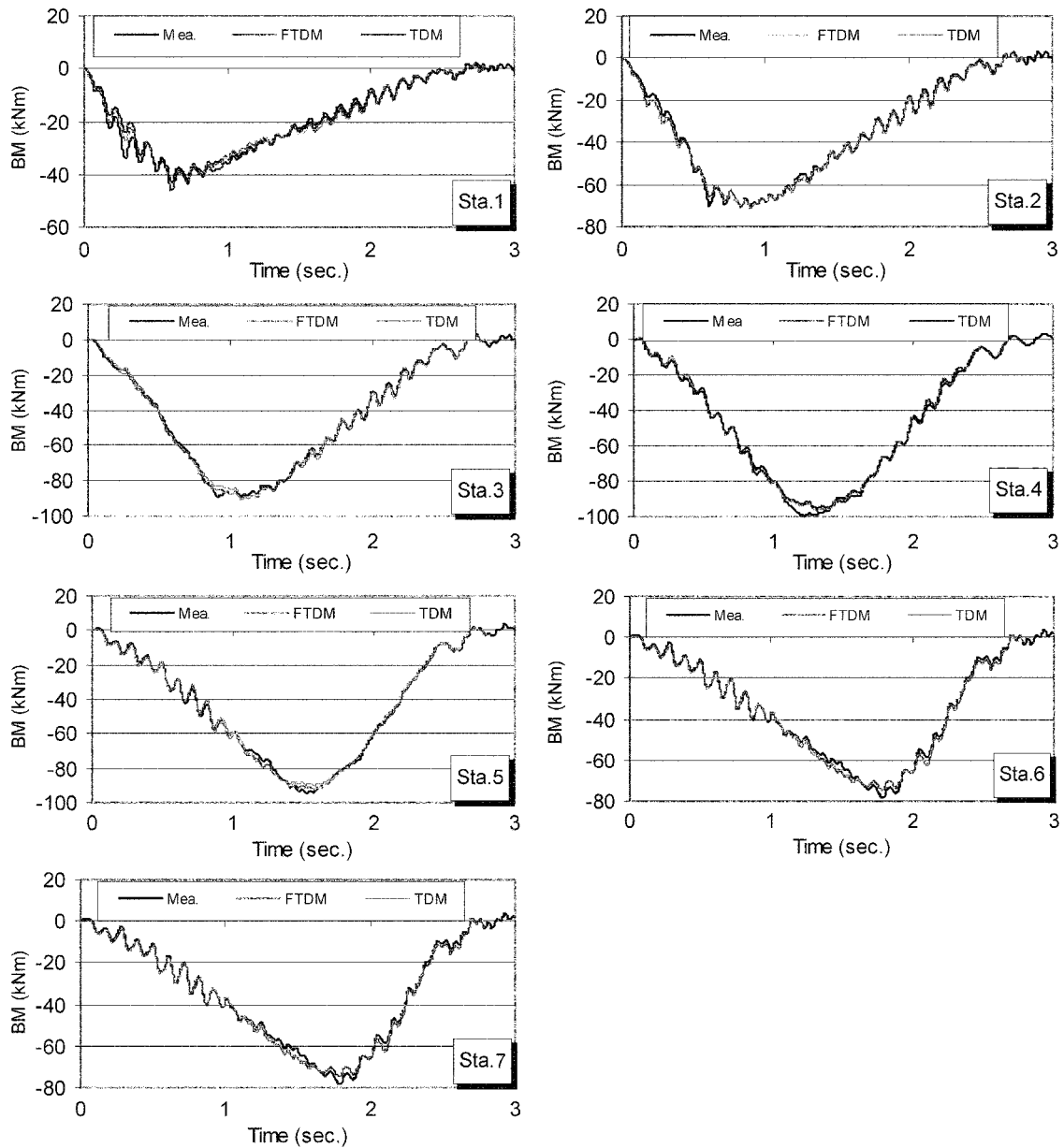
Fig. 8 Bending moments by FTDM & TDM using SVD

Fortunately, the identified result is finally acceptable in the case of 15 Units for the FTDM. However, when using the SVD the situation is completely changed. The original ineffective FTDM becomes effective when the speed is 5 Units only. The original higher RPE becomes a small RPE when the speed is 10 Units. When the vehicle moves at 15 Units the identification accuracy is also improved and better than that by using the PI technique. It seems that it is better to use the SVD technique to solve the system equation so that the FTDM can be effective and can identify the

Table 6 Effect of measuring stations on TDM and FTDM (15 Units, 250 Hz)

Station	RPE (%)							
	TDM				FTDM			
	$N_l = 3$	$N_l = 4$	$N_l = 5$	$N_l = 7$	$N_l = 3$	$N_l = 4$	$N_l = 5$	$N_l = 7$
1	*	*	*	5.43	*	*	*	4.53
	*	*	*	5.42	*	*	*	5.74
2	*	1.52	2.17	3.09	*	1.67	2.14	2.52
	*	1.48	2.17	3.08	*	2.90	34.63	2.80
3	1.26	1.42	1.82	1.80	1.24	1.50	1.71	1.87
	15.76	1.44	1.80	1.80	70.15	2.09	17.25	2.15
4	1.73	*	2.63	2.56	1.38	*	1.77	1.95
	13.39	*	2.67	2.58	77.27	*	34.68	2.08
5	1.39	1.82	1.95	1.94	1.05	1.51	1.71	1.81
	8.33	1.85	1.94	1.95	73.90	2.11	16.65	2.14
6	*	1.59	1.95	3.43	*	1.68	1.63	2.24
	*	1.56	1.98	3.44	*	2.74	32.87	2.41
7	*	*	*	4.83	*	*	*	3.17
	*	*	*	4.83	*	*	*	4.74

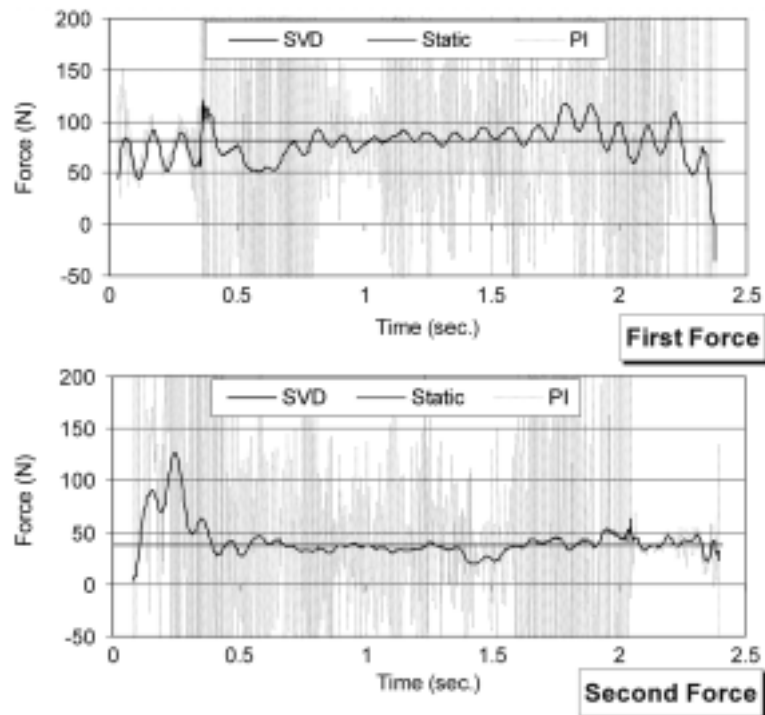Asterisk * indicates the station is not chosen.

Fig. 9 Identified forces by FTDM using SVD & PI for 5 stations

moving forces with a higher accuracy. These results also show that the identification accuracy for a faster vehicle speed is higher than that at lower vehicle speeds for both the TDM and FTDM. Fig. 8 illustrates a comparison of rebuilt responses at all 7 stations for both the TDM and FTDM. The rebuilt responses for both the TDM and FTDM agree well with the measured ones except at some localized points. In the band with a higher error, it also can be seen the FTDM results are closer to the measured bending moments.

4.4 Effect of measuring stations

To assess the effect of the measuring stations, the station number N_l was set to 2, 3, 4, 5, and 7 respectively while the other parameters MN=5, f_s = 250 Hz, c = 15 Units were not changed for any of the cases. The RPE values when using the SVD and the PI technique are given in Table 6. When using the PI technique, the underlined RPE data show that the TDM requires at least three, but best four measuring stations to obtain the two correct moving forces. However, the FTDM should have at least one more measuring station than when using the TDM, i.e. 4, to obtain the same number of moving forces. However, the RPE errors are increased obviously when the measuring station number is equal to 5 for the FTDM. This is because the addition of the fifth station is placed on the $1/2L$ point, which is a node for the second and fourth modes of the supported beam. Nevertheless, when N_l = 7, i.e., two more stations are put at the $1/8L$ and $7/8L$ respectively, the RPE values for the FTDM recover normal level to within 10%. This indicates that the FTDM is sensitive to the locations of measuring stations, and they should be selected carefully. In general, for the TDM and FTDM, the identification accuracy increases with the increase in the measuring station number, but if the increased station is put on any node of vibration modes, the identified results will be worse, especially in the case of the FTDM.

According to the data in Table 6, when the station number is equal to or bigger than four, there is almost no difference in the RPE values for the TDM, whether using the SVD or using the PI. When the station number equals three, using the SVD can dramatically improve the identification accuracy. The same situation also applies for the FTDM when the station number equals three and five. Fig. 9 illustrates the comparison between the identified first forces and between the second forces by the FTDM when using the SVD and the PI technique respectively when selecting the five measuring stations. Obviously, the FTDM failed to identify the two moving forces when using the PI to solve the system equation. However, if using the SVD the FTDM can effectively identify the two moving forces and the identification accuracy is acceptable. This shows that both the TDM and FTDM can effectively identify the two moving forces when using the SVD technique to solve the over-determined set of system equations. Particularly in the case of the FTDM, it is really important to adopt the SVD to solve the set of system equations.

5. Conclusions

The time domain method (TDM) and frequency-time domain method (FTDM) for identifying the axle force history of a moving vehicle on a bridge have been presented. A bridge-vehicle system model was constructed and used for laboratory experiments to test moving force identification methods. A series of experiments making measurements of bending moment responses caused by a vehicle moving across the model bridge were conducted. Comparative studies of moving force

identification methods have been carried out. The effects of bridge-vehicle system parameters such as sampling frequencies, numbers of mode considered, vehicle speeds, the numbers of measuring station and their locations have been investigated. The singular value decomposition (SVD) solution and the pseudo-inverse (PI) solution as used for both the time domain method and the frequency-time domain method have been compared. The following conclusions are drawn: 1) Both the TDM and FTDM are successful for the moving force identification from the measured bending moment responses caused by the vehicle moving across a bridge. 2) The effects of bridge-vehicle system parameters on the TDM and FTDM obviously depend on the solution to the over-determined system equation. 3) The use of the SVD technique can effectively improve the identification accuracy for both the TDM and the FTDM, particular for the FTDM. 4) The SVD technique is recommended as the better solution for the over-determined system equation cases involved in both the TDM and FTDM.

All the above findings are important for the further development of moving force identification systems (MFIS) to acquire real data in the field, and it can be concluded that the TDM and FTDM should be accepted as practical methods to be incorporated into the MFIS if the SVD technique is adopted.

Acknowledgements

References

Bendat, J.S. and Piersol, A.G. (1993), *Engineering Application of Correlation and Spectral Analysis*, 2nd Edition, John Wiley, New York.

Cao, X. Sugiyama, Y. and Mitsui, Y. (1998), "Application of artificial neural networks to load identification", *Comput. Struct.*, **69**, 63-78.

Chan, T.H.T., Law, S.S. and Yung, T.H. (2000a), "Moving force identification using an existing prestressed concrete bridge", *Eng. Struct.*, **22**, 1261-1270.

Chan, T.H.T. and Yung, T.H. (2000b), "A theoretical study of force identification using prestressed concrete bridges", *Eng. Struct.*, **23**, 1529-1537.

Chan, T.H.T., Yu Ling and Law, S.S. (2000c), "Comparative studies on moving force identification from bridge strains in laboratory", *J. Sound Vib.*, **235**(1), 87-104.

Fryba, L. (1972). *Vibration of Solids and Structures under Moving Loads*", Noordhoff International Publishing, Prague.

Gloub, G.H. and Van Loan, C.F. (1996), *Matrix Computations*, 3rd Edition, The Johns Hopkins University Press, London.

Law, S.S., Chan, T.H.T. and Zeng, Q.H. (1997), "Moving force identification: a time domain method", *J. Sound Vib.*, **201**, 1-22.

Law, S.S., Chan, T.H.T. and Zeng, Q.H. (1999), "Moving force identification-a frequency and time domain analysis", *J. Dynamic System, Measurement and Control*, **121**, 394-401.

Lindfield, G. and Penny, J. (1995), *Numerical Methods Using Matlab*, Ellis Horwood Limit, London.

Press, W.H., Teukolsky, S.A., Vetteling, W.T. and Flannery, B.P. (1996), *Numerical Recipes in Fortran 90: The Art of Parallel Scientific Computing*, 2nd Edition, volume 2 of Fortran numerical recipes, Cambridge University Press, England.

Starkey, J.M. and Merrill, G.L. (1989), "On the ill-conditioned nature of indirect force-measurement techniques", *The Int. J. Analytical and Experimental Modal Analysis*, **14**(3), 103-108.

Stevens, K.K. (1987), "Force identification problems-an overview", *Proc. SEM Spring Conf. on Experimental Mechanics*, 838-844.

Tang, X.J. (1990), "Precision problems of dynamic load identification in time domain", *J. Dalian University of Technology*, **30**(1), 29-38.

Timoshenko, S.P., Young, D.H. and Weaver, W. (1974), *Vibration Problems in Engineering*, Wilery, New York.